Appendix D

SUPPLEMENTARY MATERIALS FOR PHONON TRANSMISSION COEFFICIENTS AT SOLID INTERFACES

D.1 Overview

The supplementary information contains additional information on our computational approach as well as the details about experiments and modeling. Section D.2 presents transmission coefficients for all polarizations from both sides, followed by Section D.3 showing the original raw TDTR data along with the BTE fitting results. Sections D.4 & D.5 provide details about experimental measurments and modeling, respectively.

D.2 Transmission coefficients for all polarizations

In the main text, we only show the transmission coefficient from Si to Al for longitudinal phonons for the three samples. Here, in Figs. D.1, D.2 and D.3, we plot the transmission coefficient profiles as a function of phonon frequency and wavelength from both sides of the materials for each polarization with a clean interface, with a native oxide layer and with a thermally grown oxide layer. The color intensity indicates the likelihood that a single transmission coefficient curve passing through a particular point at a given phonon frequency is able to simultaneously explain all of the experimental data. We emphasize that the only fitting parameters are the transmission coefficients from Si to Al for the three polarizations. All other transmission and reflection coefficients are determined from detailed balance and energy conservation.(*79*)

For the clean interface, the only constraint used in the fitting process is the smoothness of the profile. In particular, note that we do not enforce any type of mono-

tonicity or shape requirement on the coefficients other than smoothness. For the native oxide interface, we additionally require that the transmission coefficients of the native oxide interface do not exceed the values for the clean interface. Similarly, the transmission coefficients of the thicker oxide interface should always be smaller than those of the native oxide interface.

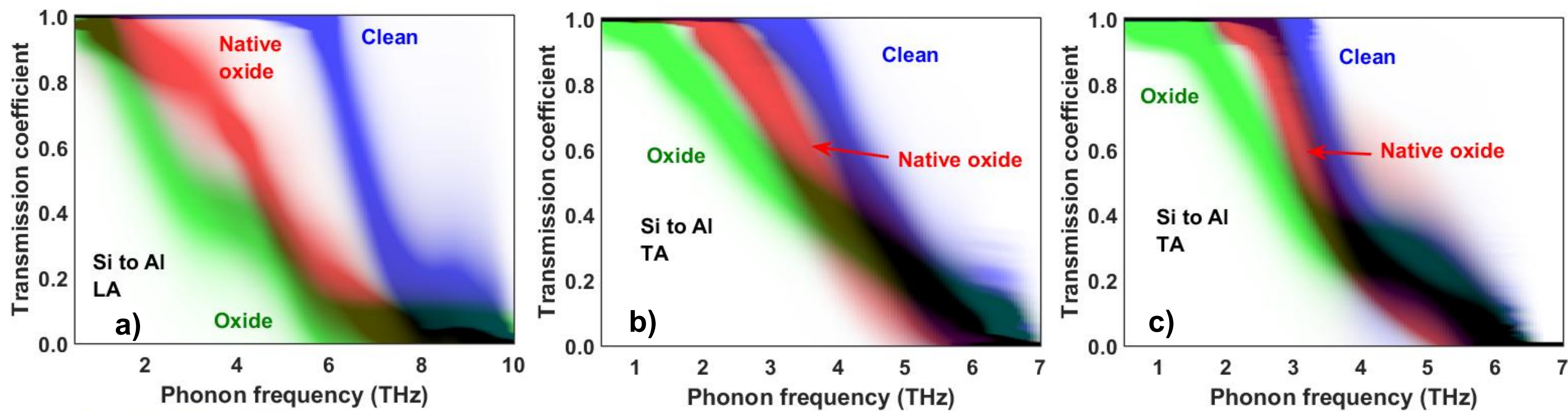

Figure D.1: Transmission coefficients from Si to Al versus phonon frequency for different polarizations measured from Al/Si sample with three different interfaces studied in this work. The intensity of the shaded region corresponds to the likelihood that the transmission coefficient possesses a given value. We emphasize that the transmission coefficients for the three polarizations are the only fitting parameters in our calculations.

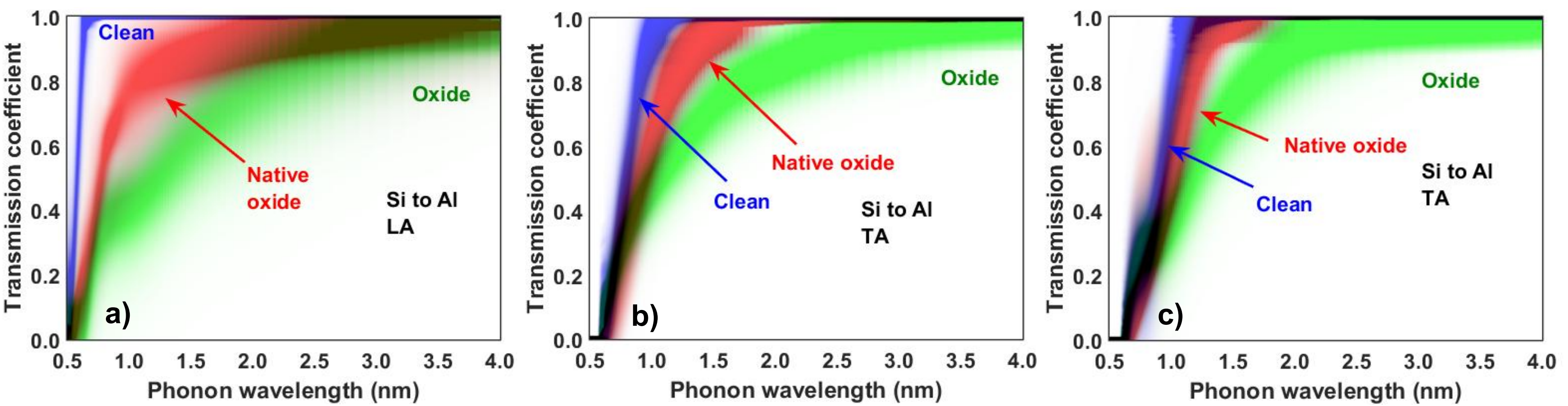

Figure D.2: Transmission coefficients from Si to Al from Fig. D.1 plotted versus phonon wavelength for different polarizations measured from Al/Si sample with three different interfaces studied in this work.

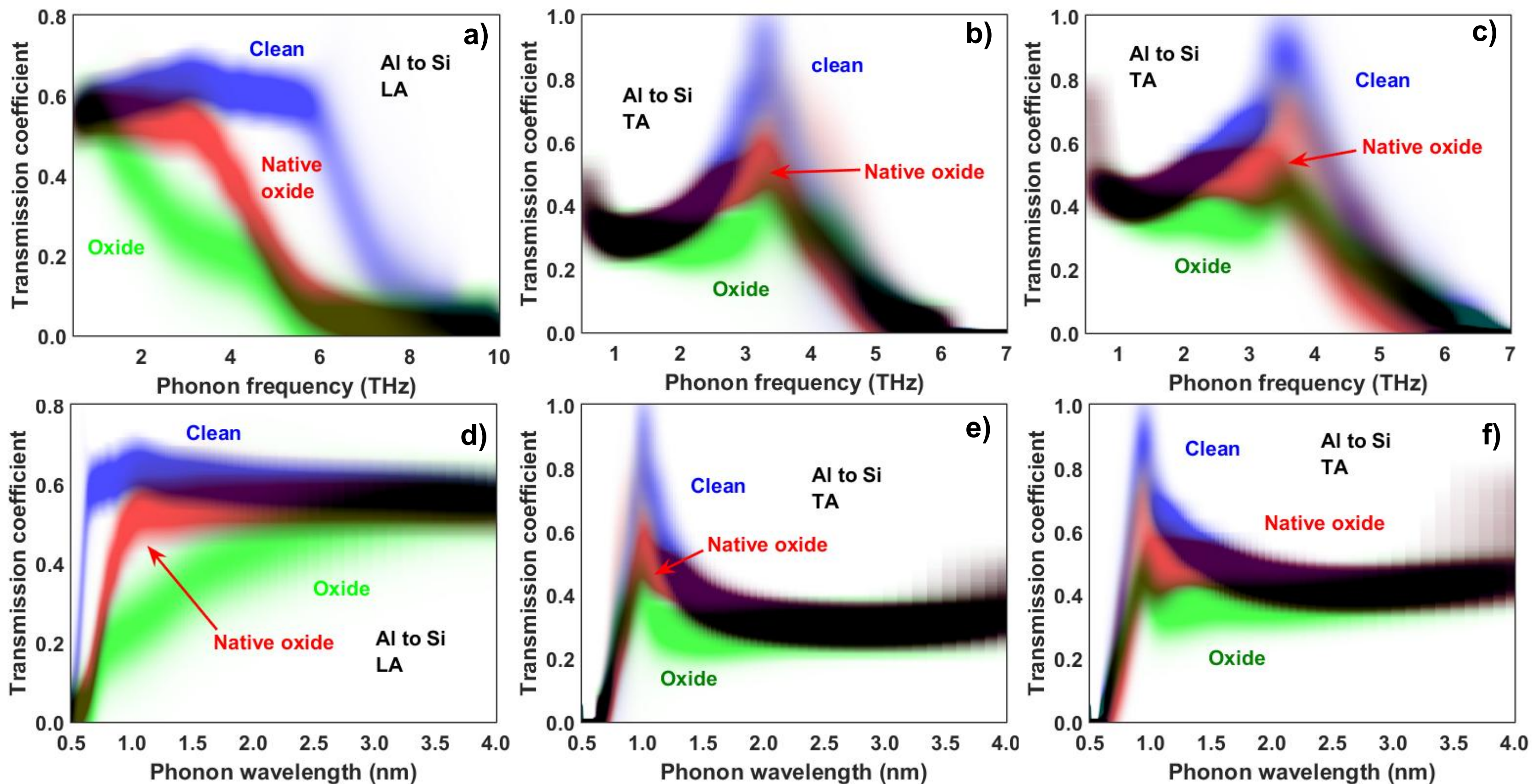

Figure D.3: Transmission coefficients from Al to Si versus (a)-(c) phonon frequency and (d)-(f) phonon wavelength for different polarizations measured from Al/Si sample with three different interfaces studied in this work, calculated using the measured values of the transmission coefficients from Si to Al shown in Fig. D.1. The increase in transmission coefficient from Al to Si at phonon frequencies less than approximately 4 THz are due to the requirements of detailed balance. Specifically, these coefficients must follow the shape of the density of states since the coefficients from Si to Al are a constant value. These coefficients are determined by the principle of detailed balance and are not free parameters.

D.3 TDTR data

In Figs. D.4 & D.5, we plot all the original raw data from the TDTR experiments used in the manuscript along with the BTE fitting results. In all the cases, we show excellent agreement between simulation and experiments.

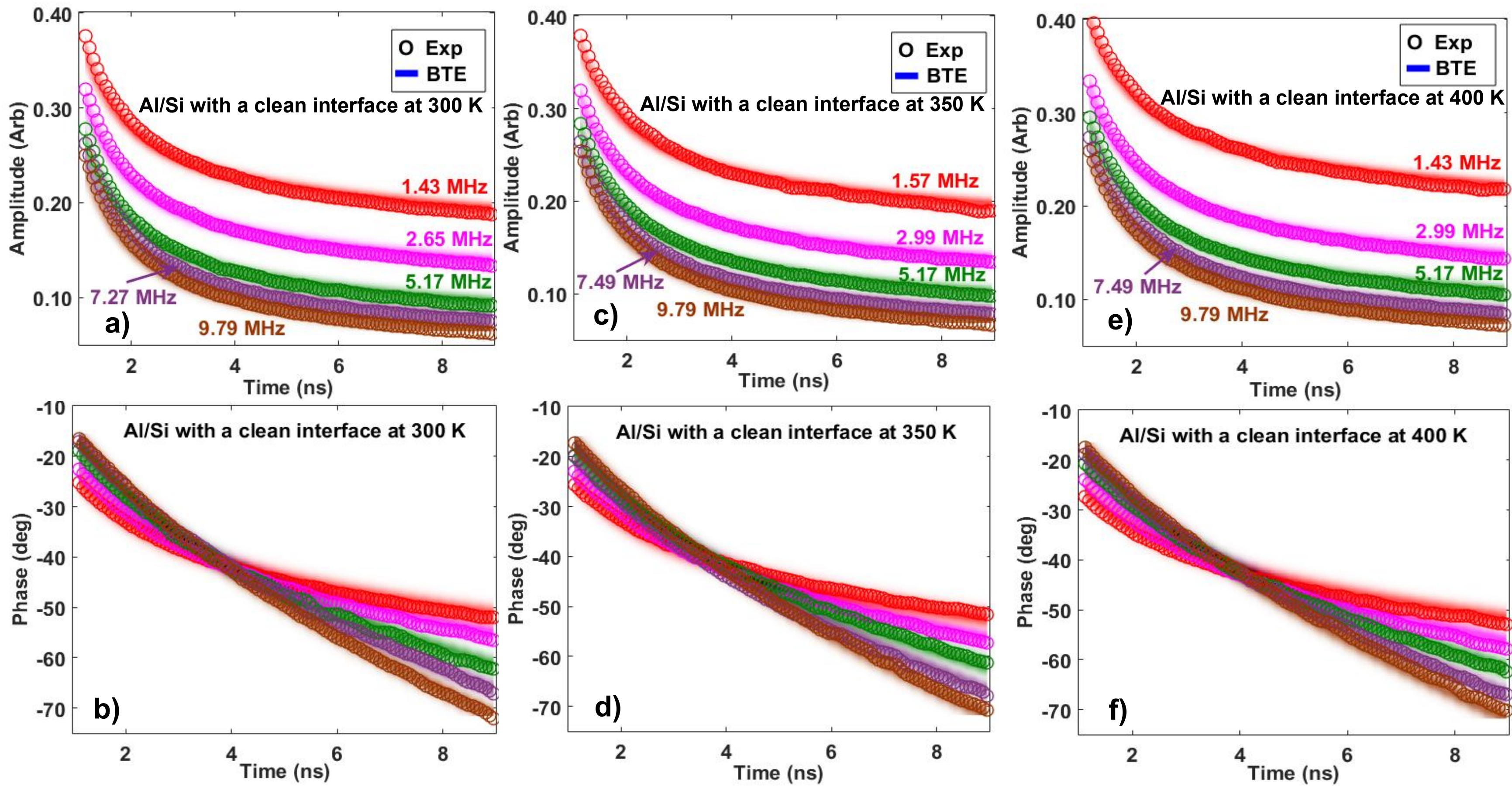

Figure D.4: Experimental TDTR data (symbols) of an Al/Si sample with a clean interface at T = 300 K, 350 K and 400 K at different modulation frequencies fit to the data from the BTE simulations (shaded regions), demonstrating excellent agreement between simulation and experiment at different temperatures.

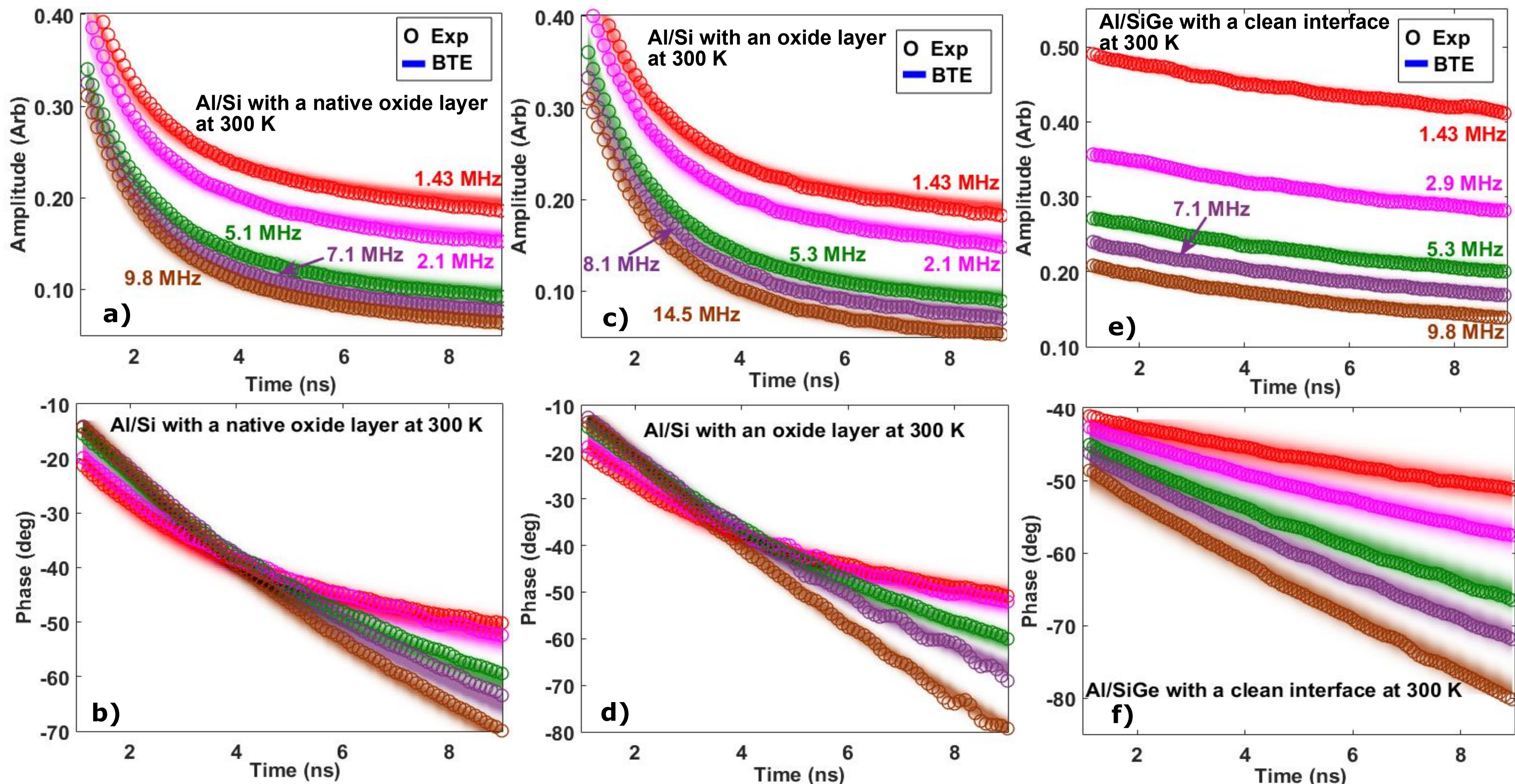

Figure D.5: Experimental TDTR data (symbols) of an Al/Si sample with a native oxidized interface, an Al/Si sample with a thermally oxidized interface, and an Al/SiGe with a clean interface at T = 300 K at different modulation frequencies fit to the data from the BTE simulations (shaded regions).

D.4 Experimental details

Sample preparation

Commercial high-purity natural Si (100) wafer and Si-Ge (1.5-2 at % Ge) wafer (100) from MTI Corp. were used in the experiments. Before coating Al on the samples, three different surface conditions of the samples were prepared. First, the native oxide was removed with buffered HF acid to obtain a clean surface of Si and SiGe. After etching, the samples were immediately put into a vacuum chamber for Al deposition. Second, the native SiO_2 layer was left in place. No further treatment was taken for this condition before Al deposition. Finally, a thermally grown SiO_2 layer as fabricated by putting the Si samples into a tube furnace for three hours. The thickness of the native SiO_2 layer and thermally grown SiO_2 layer was measured by ellipsometry and TEM to be ~ 1 nm and ~ 3.5 nm, respectively. A thin film of Al was deposited on all samples using electron beam evaporator. The thickness of the Al transducer layer was 70 nm, measured by atomic force microscopy.

TDTR measurements

The measurements are taken on two-tint TDTR. The details are available in Ref. 64. The probe diameter is 10 μm and the pump diameter is 60 μm. Both beam sizes are measured using a home-built two-axis knife-edge beam profiler. With 60 μm pump heating size, the heat transfer problem can be treated as one-dimensional. All the measurements at $T = 300$ K are performed under ambient conditions, and the additional measurements at $T = 350$ and 400 K are performed in an optical cryostat (JANIS ST-500) under high vacuum of 10^{-6} torr.

TEM images

The TEM samples were prepared by standard FIB lift-out technique in the dual beam FE-SEM/FIB (FEI Nova 600). To protect the top surface, a Pt layer with thickness ~ 300 nm was deposited with electron beam evaporation followed by

another Pt layer with thickness ~ 3-4 μm by Ga ion beam. The lamella was cut parallel to the chip edge which was aligned to the wafer flat edge during initial cutting in TDTR sample preparation. As a result, the cutting surface normal was along (110) direction and all the TEM images were taken parallel to the Si (110) crystallographic zone axis. High resolution transmission electron microscopy (HRTEM) analyses were carried out in a FEI Tecnai TF-20 TEM/STEM at 200 kV. To avoid damage from the high energy electron beam, the beam exposure on region of interest was minimized especially at high magnification during operation.

D.5 Ab-initio properties and modeling details

Point defect scattering in SiGe

For SiGe, the mass difference scattering rate is calculated using the Tamura formula,(*184*) given by

$$\tau^{-1} = \frac{\pi}{6} V_0 m_0 \omega^2 D(\omega), \tag{D.1}$$

where ω is phonon frequency, $D(\omega)$ is the phonon density of states per unit volume, and V_0 is the volume per atom. $m_0 = \sum_i f_i (1 - m_i/\bar{m})^2$ is a measure of the mass disorder, f_i and m_i are the concentration and the atomic mass of species i, respectively, and $\bar{m}$ is the average mass for the given composition. The Tamura formula has been proven to effectively calculate the impurity scattering in SiGe with different Ge concentration.(*185*) The values of all the constants in Eq. D.1 are tabulated in Table D.1

We have sent the SiGe wafer to the third party, Thermotest, for bulk thermal conductivity measurements. The measured value, using transient plane source method on a bulk sample, is 50.7 ± 0.5 W/m-K. Using the measured value, we are able to obtain the Ge concentration to be about ~ 2 at % based on calculations with the Tamura formula while the measured Ge concentration using Energy Dispersive X-ray Spectrometry is ~ 1.5 at %, which gives SiGe thermal conductivity around

~ 58 W/m-K. These differences in atomic concentration have only a minimal effect on the transport calculations and have been incorporated in the uncertainty of BTE simulations in Fig. 5.12 of the main text.

Al thermal conductivity

We assume a constant MFP for all modes in Al; the value $\Lambda_{Al} = 60$ nm is chosen to yield a lattice thermal conductivity $k \approx 123$ W/m-K so that no size effects in the thin film occur. Although the literature value of Al thermal conductivity is about 230 W/m-K, we verified that the resulting surface temperature decay curves by using these two Al thermal conductivities in the TDTR diffusion model could not be distinguished as shown in Fig. D.6. Since the transmission coefficients are extracted by fitting our model to the data, if a parameter in the model has little effect on the results of the model, then it cannot affect the measured transmission coefficients. Here, we demonstrate that the calculations are completely insensitive to Al thermal conductivity, provided that it is larger than ~ 30 W/m-K. Therefore, our choice of Al thermal conductivity has no impact on our results.

The relaxation time for each mode is then obtained through $\tau_\omega = \Lambda_{Al}/v_\omega$. We also verified that the particular value of the Al MFP does not affect the results. Note that although the Al MPF is a constant, the dispersion of Al is directly from the first-principle calculations, and the transmission coefficients depend heavily on the density of states and phonon group velocity in both metal and substrate. Therefore, Al is still modeled with a spectral phonon BTE.

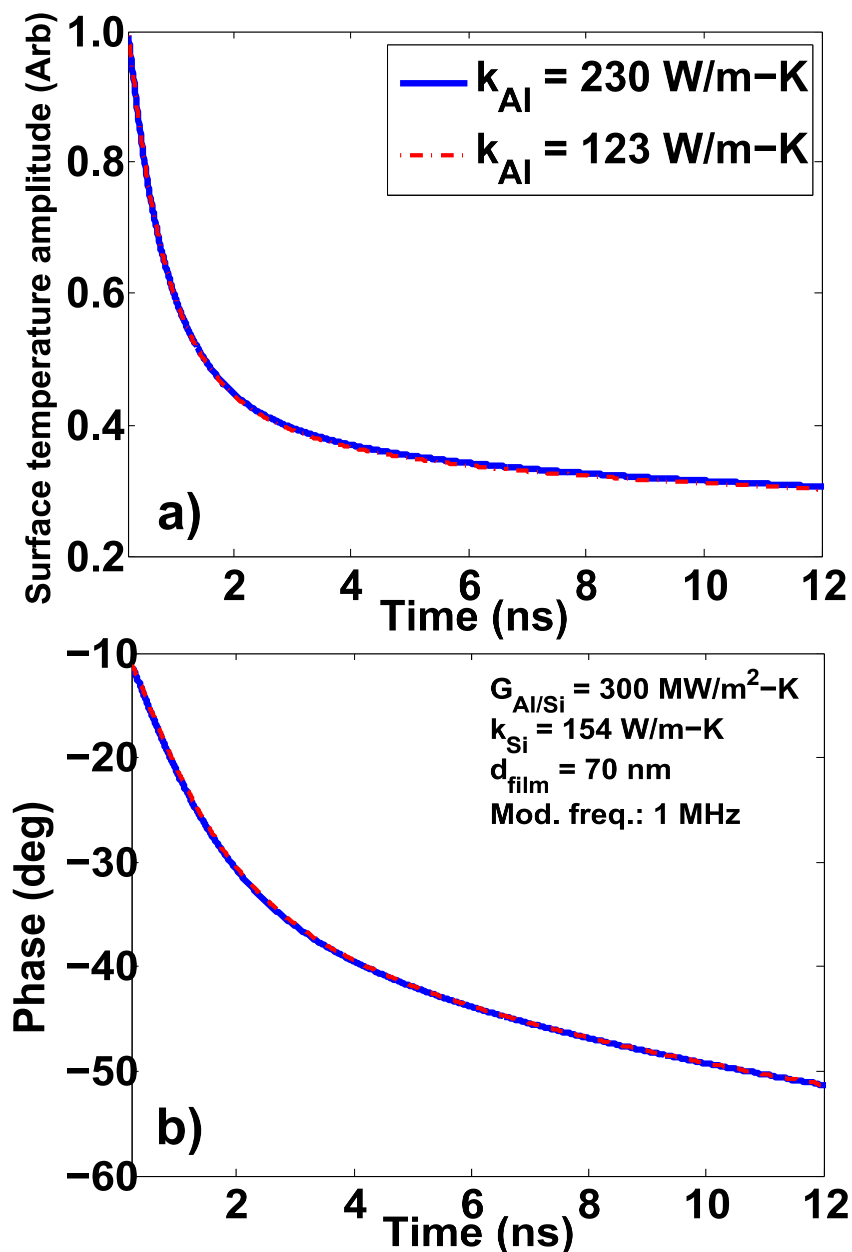

Figure D.6: Calculated transient surface temperature (a) amplitude and (b) phase for Al on Si using a two-layer diffusive model with Al thermal conductivity to be 230 W/m-K (solid blue line) and 123 W/m-K (dash-dotted red line). The surface temperature response is not sensitive to the change of Al thermal conductivity from 230 W/m-K to 123 W/m-K.

Table D.1: All the constants appearing in the BTE models and the fitting process are given in the following table.

Bulk thermal properties	
Al heat capacity (J/m^3-K):	2.41×10^6
Al lattice thermal conductivity (W/m-K):	123
Al total thermal conductivity (W/m-K):	230
Si heat capacity (J/m^3-K):	1.63×10^6
Si thermal conductivity (W/m-K):	155
SiGe heat capacity (J/m^3-K):	1.63×10^6
SiGe thermal conductivity (W/m-K):	51
Electronic thermal properties in Al	
Heat capacity (J/m^3-K):	4.11×10^4
Thermal conductivity (W/m-K):	203
Electron-phonon coupling coefficient g (W/m^3-K):	2.1×10^{17}
Constants in Tamura formula	
Volume per Si atom V_0 (nm^3):	0.02
Measure of the mass disorder m_0:	0.0568
Transducer film thickness	
Al/Si with a clean interface (nm):	69
Al/SiGe with a clean interface (nm):	72
Al/Si with a native oxidized interface (nm):	70
Al/Si with a thermally-grown oxidized interface (nm):	70
Other constants	
Optical penetration depth δ (nm):	10
Laser repetition frequency (MHz):	76